An Introduction to Integrated Optics

HERWIG KOGELNIK, FELLOW, IEEE

Abstract—**An introduction is given to the principles of integrated optics and optical guided-wave devices. The characteristics of dielectric waveguides are summarized and methods for their fabrication are described. An illustration is given of recent work on devices including directional couplers, filters, modulators, light deflectors, and lasers.**

I. INTRODUCTION

IT IS now five years since the name "integrated optics" was coined [1], and there are now research activities in this field in an increasing number of industrial, governmental, and university laboratories. For the interested reader there is already available a good collection of survey articles [2]–[5] which review both the history and the fundamentals of this new discipline. The purpose of this paper is to give the reader an introduction to integrated optics and an illustration of present day activities. While no attempt is made to present a complete survey, we will try to collect the major thoughts and arguments which have motivated and stimulated work in this field.

Clearly, one impetus stems from the promise of optical-fiber transmission systems [6] which is rooted in the recent achievement of low transmission losses in optical fibers. Integrated optics may one day provide circuits and devices for the repeaters of these systems, in particular, when higher transmission speeds are envisaged, or it may offer possibilities for wavelength multiplexing or switching of optical signals. The spectral range of interest is, therefore, in the visible and near infrared where fiber losses are low. There is also activity at 10.6 μm, the wavelength of the CO_2 laser where device improvements are needed for communications and the processing of laser radar signals.

The area defined by the name "integrated optics" has expanded gradually, and it now includes all exploration towards the use of guided-wave techniques to fabricate new or improved optical devices. With this, one associates compact and miniaturized devices, and hopes that small size will lead to better reliability, better mechanical and thermal stability, and to lower power consumption and drive voltages in active devices. Of course, there is also the promise of integration, i.e., that one will be able to combine several guided-wave devices and form more complicated circuits on a common substrate or chip. However, some of the new guided-wave devices, lasers or modulators for example, may well be able to compete on their individual merits with their bulk-optical counterparts.

The waveguides used in integrated optics are dielectric waveguides, usually in the form of a planar film or strip with a refractive index higher than that of the substrate. The guiding mechanism is total internal reflection. Typical refractive index differences are 10^{-3}–10^{-2}, and guide losses of less than 1 dB/cm are desirable.

The fabrication techniques are reminiscent of the technology of electronic integrated circuits. Planar structures predominate and photolithographic techniques are employed. Naturally there are new requirements, a particularly stringent one being the need for an edge roughness smaller than 500 Å to keep light scattering losses to a tolerable level.

The devices we talk about are the counterparts of familiar microwave and optical devices. They are couplers, junctions, directional couplers, filters, wavelength multiplexers, and active devices such as modulators, switches, light deflectors, and lasers. Later sections will illustrate some of the recent device work in more detail, but first we will give a brief survey of the characteristics of dielectric waveguides.

II. DIELECTRIC WAVEGUIDES

The properties of dielectric waveguides are discussed in great detail in the cited review articles [2]–[5] as well as in recent textbooks on this subject [7]–[9]. The planar slab waveguide is one of the simplest waveguide structures and it is also one of the most commonly used in integrated optics. We shall use it in the following to illuminate the principal characteristics of dielectric guides.

A. The Asymmetric Slab Waveguide

The planar asymmetric slab guide structure is illustrated in Fig. 1. We have a film of thickness f (usually a fraction of a micrometer) and of refractive index n_f, and a cover and substrate material of lower index n_c and n_s respectively, so that

$$n_f > n_s \geq n_c. \tag{1}$$

The structure is called asymmetric when $n_s \neq n_c$ and symmetric when $n_s = n_c$.

In dielectric guides, we distinguish between two types of electromagnetic modes, guided modes and radiation modes. Following Tien [4] we can use ray arguments to distinguish between these types. This is illustrated in Fig. 2, where we have shown light rays incident on the structure with increasing angles of incidence. In Fig. 2(a) the incident ray penetrates through the structure. On its passage it is refracted according to Snell's law:

$$n_f \sin \Theta_f = n_s \sin \Theta_s = n_c \sin \Theta_c. \tag{2}$$

The light escapes again from the structure in this situation

Manuscript received March 28, 1974; revised August 13, 1974.
The author is with Bell Laboratories, Holmdel, N. J. 07733.

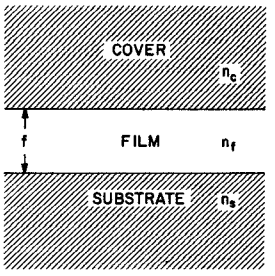

Fig. 1. Schematic of asymmetric dielectric slab waveguide.

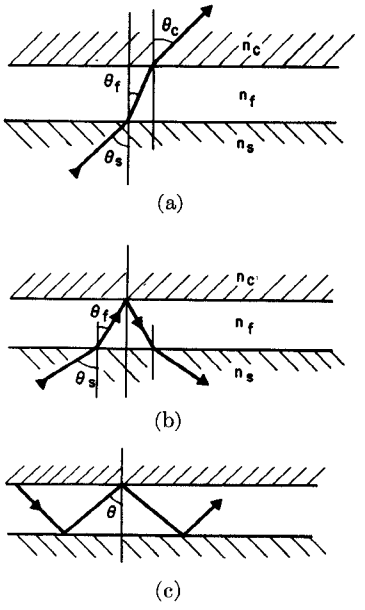

Fig. 2. Ray pictures illustrating radiation modes (a), substrate modes (b), and guided modes (c) in a dielectric slab waveguide.

which we associate with a radiation mode. This is also the case for the situation depicted in Fig. 2(b) where the light is incident at a somewhat larger angle Θ_c. We have, still, refraction at the substrate–film interface, but at the film–cover interface we surpass the critical angle and the light is totally reflected and escapes through the substrate. In Fig. 2(c) the angle $\Theta \equiv \Theta_f$ is still larger, surpassing the critical angle both at the film–substrate and film–cover interfaces resulting in total internal reflection at both locations. The light is trapped in the film which corresponds to a guided mode of the structure.

According to this zigzag model a guided mode is represented by plane waves traveling in a zigzag path through the film. The modal fields propagate like exp $(-j\beta z)$ in the z direction with a propagation constant β related to the zigzag angle θ by

$$\beta = kn_f \sin\theta \tag{3}$$

where $k = 2\pi/\lambda = \omega/c$, λ is the free-space wavelength, ω the angular frequency of the light, and c the velocity of light. Equation (3) and the critical angle produce bounds for β which are

$$kn_s < \beta < kn_f. \tag{4}$$

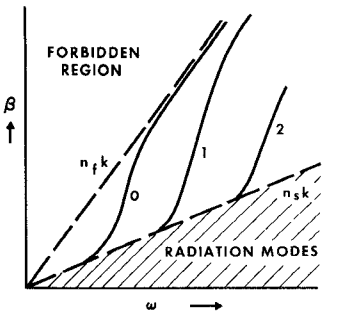

Fig. 3. Typical ω–β diagram for dielectric slab waveguides. Three discrete guided modes are shown.

The lower bound is reached at cutoff, i.e., at the critical angle and the upper bound is approached for glancing angles of incidence θ. Fig. 3 shows a typical ω–β diagram for the first three modes (labeled 0, 1, and 2) which indicates the variation of β with frequency ω (or relative film thickness). Typically, we have a discrete spectrum of guided modes and a continuous spectrum of radiation modes.

In discussing dielectric waveguides it is often convenient to define an effective guide index N which is related to the propagation constant β by

$$N = \beta/k = n_f \sin\theta. \tag{5}$$

Its values are bounded by the substrate and film indices

$$n_s < N < n_f. \tag{6}$$

We will mention one use of this effective index later in connection with strip guides.

While the field of a guided mode can be viewed as a zigzagging plane wave in the film, we have evanescent fields in the substrate and the cover which decay as exp $(-\gamma x)$. The expressions for the decay constants γ_s and γ_c follow from Maxwell's equations as

$$\begin{aligned} \gamma_s^2 &= k^2(N^2 - n_s^2) \\ \gamma_c^2 &= k^2(N^2 - n_c^2) \end{aligned} \tag{7}$$

where the subscripts s and c refer to substrate and cover, respectively.

We can use the zigzag model to determine the propagation constant of a guided mode if we bear in mind the phase shift that occurs on total reflection of plane waves. For phase shifts $2\phi_s$ and $2\phi_c$ at the film–substrate and film–cover interfaces we have the formulas [4]

$$\begin{aligned} \tan^2\phi_s &= (N^2 - n_s^2)/(n_f^2 - N^2) \\ \tan^2\phi_c &= (N^2 - n_c^2)/(n_f^2 - N^2) \end{aligned} \tag{8}$$

for waves with TE polarization, i.e., for electric fields perpendicular to the plane of incidence.

Fig. 4 shows the zigzag model and our choice of the coordinate system. To obtain the self-consistent solution corresponding to a waveguide mode we require that the phase shifts accumulated during one complete zigzag add up to a multiple of 2π. The phase shift corresponding to a single transversal of the film (in the x direction) is

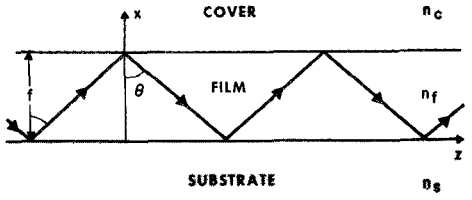

Fig. 4. Zigzag wave picture for slab waveguides.

TABLE I
ASYMMETRY MEASURES FOR TE MODES (a_E) AND TM MODES (a_M)

Waveguide	n_s	n_f	n_c	a_E	a_M
GaAlAs, double heterostructure	3.55	3.6	3.55	0	0
Sputtered glass	1.515	1.62	1	3.9	27.1
Outdiffused $LiNbO_3$	2.214	2.215	1	881	21,206

$kn_f f \cos\theta$. For a complete zigzag we have

$$2kn_f f \cos\theta - 2\phi_s - 2\phi_c = 2m\pi. \tag{9}$$

This is the dispersion relation which determines $\beta(\omega)$. Approximate solutions for this are available [10], but for the general case, we have to resort to a numerical evaluation. To make the numerical results broadly applicable it is useful to introduce a series of normalizations for the guide parameters. The first is the normalized film thickness V defined as

$$V = k \cdot f \cdot (n_f^2 - n_s^2)^{1/2} \tag{10}$$

and the second is a measure of the asymmetry of the structure [11] given by

$$a = (n_s^2 - n_c^2)/(n_f^2 - n_s^2). \tag{11}$$

This measure applies to the TE modes and ranges in value from zero for perfect symmetry ($n_s = n_c$) to infinity for strong asymmetry ($n_s \neq n_c$ and $n_s \to n_f$). As an illustration we list in Table I the refractive indices of some practical guide structures together with the asymmetry measure (a_E). The third is the definition of a "normalized guide index" b related to the effective index N by

$$b = (N^2 - n_s^2)/(n_f^2 - n_s^2) \tag{12}$$

which takes on zero value at cutoff and has a maximum value of unity. Fig. 5 shows a plot of the index b as a function of the normalized film thickness V (which is also proportional to ω) for various degrees of asymmetry in the guide structure. Values for the first three TE modes are plotted. This plot is a close relative of the ω–β diagram, in particular as we have a simple linear relation

$$N \approx n_s + b(n_f - n_s) \tag{13}$$

when the difference between the film and substrate indices is small ($n_f \approx n_s$). In this latter case the chart of Fig. 5 can also be applied to TM modes as long as we define the asymmetry measure a in a somewhat different manner, namely by [11]

$$a = \frac{n_f^4}{n_c^4} \cdot \frac{n_s^2 - n_c^2}{n_f^2 - n_s^2}. \tag{14}$$

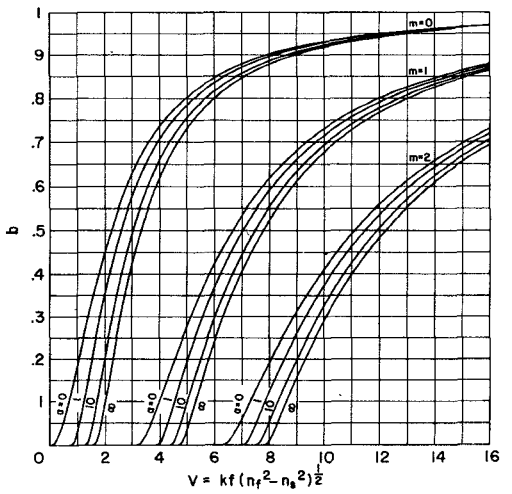

Fig. 5. Guide index b as a function of normalized frequency V for slab waveguides with various degrees of asymmetry. (From [11].)

Table I includes values for this measure under a_M.

Fig. 5 reflects the fact that the fundamental mode of a symmetric guide has no cutoff. The cutoff value V_0 for the fundamental mode of an asymmetric guide is obtained from the dispersion equation as

$$V_0 = \tan^{-1} a^{1/2}. \tag{15}$$

We can write this in terms of film thickness and wavelength in the form

$$(f/\lambda)_0 = \frac{1}{2\pi(n_f^2 - n_s^2)^{1/2}} \tan^{-1} a^{1/2}. \tag{16}$$

In an oversized waveguide many modes are allowed to propagate, with the number m of allowed guided modes given by

$$m = \frac{2f}{\lambda}(n_f^2 - n_s^2)^{1/2} \tag{17}$$

which is independent of the degree of asymmetry.

B. Effective Guide Thickness

In Fig. 4 we have associated the drawn arrows with the wave normals of zigzagging plane waves. When we investigate phenomena in the waveguide which involve the exchange or flow of energy we have to go one step further and consider the behavior of wave packets or rays. These are indicated in Fig. 6. Burke [12] has pointed out that this ray picture should include the Goos-Haenchen shifts which occur on total reflection from the film–substrate and film–cover boundaries. These ray shifts of $2z_s$ and $2z_c$ are included in the figure. One can show [13] that this shift of the reflected wave packet is related to a derivative of the phase shifts ϕ_s and ϕ_c:

$$z_s = d\phi_s/d\beta = \frac{1}{\gamma_s}\tan\theta$$

$$z_c = d\phi_c/d\beta = \frac{1}{\gamma_c}\tan\theta \tag{18}$$

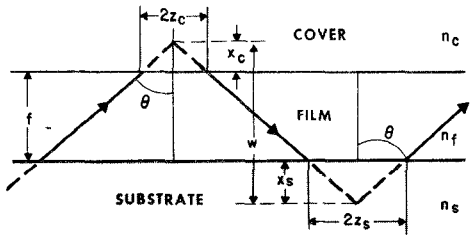

Fig. 6. Zigzag wave picture for slab waveguides with Goos–Haenchen shifts included.

where the expressions given on the right-hand side apply to the TE modes. This is the spatial analog of the $d\omega/d\beta$ relation for the group velocity which follows from consideration of timelike wave packets. As a consequence of this shift the ray appears to penetrate into substrate and cover as indicated in the figure. We calculate the apparent penetration depths x_s and x_c from (18) as

$$x_s = 1/\gamma_s$$
$$x_c = 1/\gamma_c. \tag{19}$$

As the appearance of the decay constants γ suggests, there is a close relation between this ray penetration and the existence of evanescent fields in substrate and cover.

As a consequence of the ray penetration the waveguide appears to possess an effective thickness w

$$w = f + 1/\gamma_s + 1/\gamma_c \tag{20}$$

which is larger than its actual thickness f and which always turns up as a characteristic parameter when questions of energy exchange are involved.

Fig. 7 gives a plot for the normalized guide thickness

$$W = kw(n_f^2 - n_s^2)^{1/2} \tag{21}$$

for the TE_0 modes of asymmetric slab guides for various degrees of asymmetry [11]. This figure also gives an idea of the degree of light confinment that we can achieve with a dielectric waveguide. On the chart we observe a broad minimum of $W = 4.4$ at $V = 2.55$ occurring for $a = \infty$. This implies a minimum achievable effective width $w_{\min}$ of

$$w_{\min}/\lambda = 0.7 \cdot (n_f^2 - n_s^2)^{-1/2} \tag{22}$$

which is a function of the film–substrate index difference. For $n_s = 1.5$ and $n_f = 1.6$ we get $w_{\min} \approx 1.3\lambda$.

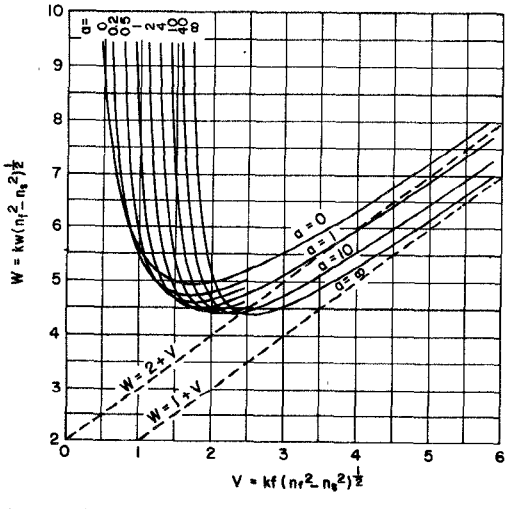

Fig. 7. Normalized effective guide thickness W as a function of normalized frequency V for slab guides with various degrees of asymmetry. (From [11].)

C. Strip Guides

A planar slab guide provides no confinment of the light in the film plane. For some devices this confinement is not necessary, and for others it is not even desired. Examples for the latter are planar devices such as the acoustooptic light deflectors in thin-film form [14], and the planar film lenses and prisms proposed for optical data processing [15], [16]. Strip guides provide confinement in the film plane. In some active devices such as lasers and modulators this additional confinement is very desirable as it can lead to a reduction in drive voltage and power consumption. A considerable number of devices can, and some have been, made in both the planar and the strip version. An example are directional couplers which one can make by fabricating two strip guides with a close spacing, or by separating two planar slab guides by a thin layer of lower index material [17]. Generally, it appears that the planar device versions are easier to fabricate, while the strip-guide versions provide more compactness and flexibility.

Strip guides can be made in a variety of ways. Fig. 8 shows four examples of possible strip-guide (x–y) cross sections which have a typical width of a few micrometers. Fig. 8(a) shows a raised strip guide, which can be fabricated from a slab guide by masking the strip and removing the surrounding film by reverse sputtering, ion-beam etching, or chemical etching. The imbedded strip in Fig. 8(b) can be made by ion implantation through a mask. The ridge guide of Fig. 8(c) is fabricated by the same process as the raised strip but with incomplete removal of the surrounding film. The strip-loaded guide of Fig. 8(d) is formed by depositing a strip of material with lower index $n_c < n_f$ onto a slab guide. For reasons of simplicity the sketches of the figure show abrupt changes of refractive index or film thickness. However, some fabrication methods, such as diffusion through a mask lead to guides with graded transitions.

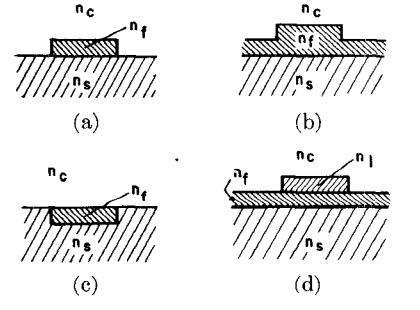

Fig. 8. Cross sections of various strip guide configurations. (a) Raised strip. (b) Embedded strip. (c) Ridge guide. (d) Strip-loaded guide.

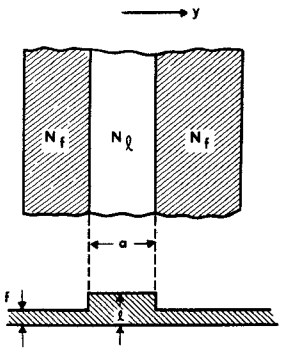

Fig. 9. Schematic illustrating the application of the effective index method to a ridge guide.

The ridge guide is, of course, a close relative of the recently reported single material fiber [18]. Both the ridge (or "rib") guide [19], [20] and the strip-loaded guide [21], [22] have been proposed because of their promise in relaxing the stringent fabrication requirements for resolution and edge smoothness. Both use a propagating surround, i.e., a surronding slab guide allowing at least one guided mode.

No exact analytic solutions for the modes of strip guides are available. Numerical calculations have been made for rectangular dielectric guides embedded in a uniform surround [23], [24], and Marcatili [10], [25] has given approximate solutions applicable to a large class of strip guides operating sufficiently away from cutoff.

The effective index method is another simple way to get some fairly good predictions for the behavior of strip guides such as the ridge and the strip-loaded guides. It has been applied to predict the characteristics of thin-film prisms and lenses [15], [16] and strip-loaded guides [22], giving good agreement with experimental results. In Fig. 9 we have sketched this method for the ridge guides. Corresponding to the ridge region on the one hand and the surround on the other we consider two unbounded slab guides of thickness l and f and normalized thickness V_l and V_f, respectively. We use these parameters to determine the corresponding guide indices b_l and b_f and the effective indices N_l and N_f, for example, via Fig. 5. To predict the guide characteristics in the y direction we consider a symmetric slab guide with a thickness equal to the ridge width a, and with substrate index N_f and film index N_l as indicated in the figure. To this "equivalent" slab guide we can apply all the results available for slab guides and arrive at estimates for quantities of experimental interest; e.g., we can determine the number of guided modes m_y allowed in the y dimension from (17), which becomes

$$m_y = \frac{2a}{\lambda}(N_l^2 - N_f^2)^{1/2} = \frac{2a}{\lambda}[(n_f^2 - n_s^2)(b_l - b_f)]^{1/2} \tag{23}$$

or we can use (21) in combination with Fig. 7 to determine the minimum effective width $w_{y\,\min}$ in the y direction from

$$W_{y\,\min} = kw_{y\,\min}(N_l^2 - N_f^2)^{1/2}$$
$$= kw_{y\,\min}[(n_f^2 - n_s^2)(b_l - b_f)]^{1/2} \approx 5. \tag{24}$$

III. THE USE OF COUPLED WAVES AND PERIODIC STRUCTURES

Many phenomena in physics and engineering can be viewed as coupled-wave phenomena. To these belong the diffraction of X-rays in crystals [26], the scattering of light by acoustic waves [27] or by hologram gratings [28], the directional coupling of microwaves [29], [30], and the energy exchange between electron beams and slow-wave structures in microwave tubes [30], [31]. In integrated optics we encounter a great variety of coupled-wave phenomena, and Yariv [32] has recently given a summary of these. They include the conversion of TE to TM modes in anisotropic waveguides [33], [34] or in magnetooptic modulators [35], or the backward scattering in distributed feedback structures of lasers [36].

Dealing with coupled-wave phenomena we usually consider two waves or modes (R and S) of a guiding structure which propagate freely and uncoupled as long as the structure is not perturbed. A perturbation of the original structure, e.g., an induced change of the refractive index of a film guide, will lead to a coupling of the two waves and an exchange of energy between them. As the interaction over distances of a wavelength is usually weak, we talk of a *slow* exchange of energy and a *slow* change of the complex amplitudes $R(z)$ and $S(z)$ of the coupled waves. Typical interaction lengths useful for integrated optics devices are between 100 μm and 1 cm. An important requirement for a significant interaction is the synchronism or "phase matching" between the two coupled waves, which, in the simplest case, is the requirement for the equality

$$\beta_R = \beta_S \tag{25}$$

of the propagation constants β_R and β_S of the two waves.

In the following discussion we will distinguish between the coupling of two guided modes and the coupling to radiation modes. Another distinction is between waves with codirectional and waves with contradirectional flow of energy.

A. Codirectional Coupling of Guided Modes

When the group velocities of R and S point in the same direction, we talk of codirectional coupling or forward scattering (or the Laue case). This is indicated in Fig. 10(a) where we have sketched the change in wave amplitudes. The usual boundary condition in this case is

$$R(o) = R_0$$
$$S(o) = 0 \tag{26}$$

i.e., a reference wave R with an incident amplitude R_0 and a scattered wave S starting with zero amplitude. For

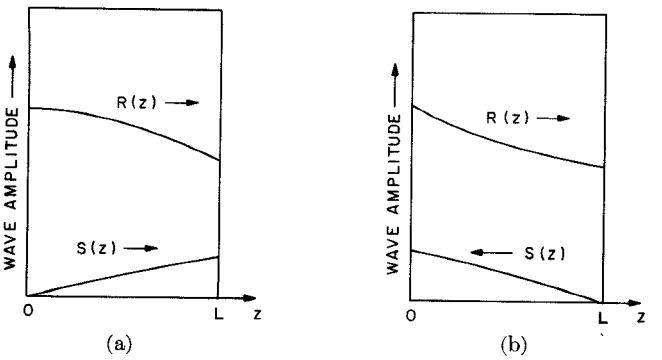

Fig. 10. Variation of coupled wave amplitudes with distance. (a) Forward scattering. (b) Backward scattering.

synchronism one gets a periodic interchange of energy described by amplitudes [26]–[32]

$$S(L) = -jR_0 \sin(\kappa L)$$
$$R(L) = R_0 \cos(\kappa L) \tag{27}$$

where κ is called the coupling constant and L is the interaction length. For this case we can get a complete transfer of power from R to S if we choose an interaction length of $\pi/2\kappa$.

The coupling coefficients depend on the particular device structure. Snyder [37] and Marcuse [9] have applied a coupled mode theory to perturbed dielectric waveguides and found that κ is proportional to an over'ap integral containing the (normalized) electric field distributions $E_R(x,y)$ and $E_S(x,y)$ of the two coupled modes. For TE modes this is of the form

$$\kappa \propto \iint dx\, dy (n^2 - n_0^2) E_R \cdot E_S^* \tag{28}$$

where $n_0(x,y)$ is the index profile of the unperturbed waveguide and $n(x,y,z)$ is the index profile of the perturbed structure. Reference [32] gives the coefficients for nonlinear interactions and for electrooptic, magnetooptic, and photoelastic modulation in dielectric waveguides.

B. Contradirectional Coupling of Guided Modes

Contradirectional coupling or backward scattering occurs when the group velocities of R and S point in opposite directions as indicated in Fig. 10(b). This is also referred to as the Bragg case. Here the usual boundary conditions are

$$R(o) = R_0$$
$$S(L) = 0 \tag{29}$$

with the scattered wave S starting with zero amplitude at the end of the interaction region. The resulting energy interchange at synchronism is described by amplitudes [26]–[28], [31], [32]

$$S(o) = jR_0 \tanh(\kappa L)$$
$$R(L) = R_0/\cosh(\kappa L). \tag{30}$$

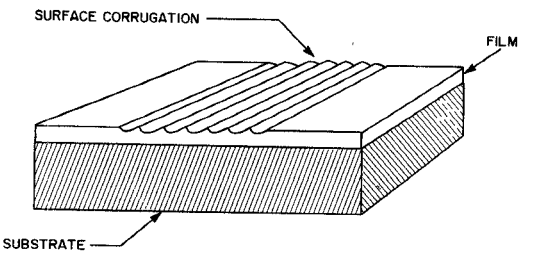

Fig. 11. Sketch of thin-film waveguide with a surface corrugation.

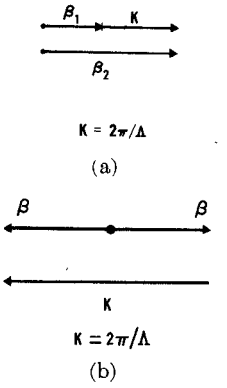

Fig. 12. Wave vector diagrams. (a) For mode matching forward scattering. (b) Backward Bragg scattering of guided modes (β) by a periodic structure (K).

The scattered wave appears on reflection from the structure.

C. Periodic Structures

Periodic structures are used in integrated optics in several forms, including films with surface corrugations and index perturbations produced by an acoustic wave [14], and for several different purposes, including light deflection [14], filtering [32], [38], [39], and for the spectral narrowing of laser output [36]. Fig. 11 shows the example of a film with a surface corrugation. The scattering of light by a periodic structure can be viewed as a coupled wave process. We can associate a grating vector K

$$K = 2\pi/\Lambda \tag{31}$$

with the structure which is related to its period Λ. The periodicity establishes synchronism between two modes with different propagation constants β_1 and β_2 if

$$\beta_2 = \beta_1 + K. \tag{32}$$

This leads to forward scattering as sketched in Fig. 12(a). The magnetooptic modulators of [35] and the mode conversion by means of acoustic waves [40] are two experiments where this method was used. The structures here can be relatively coarse with periods Λ of many micrometers

Fig. 12(b) shows the case of backward scattering where a mode of propagation constant β is coupled to a mode traveling in the opposite direction with $-\beta$. This interaction is strongest if

$$K = 2\beta. \tag{33}$$

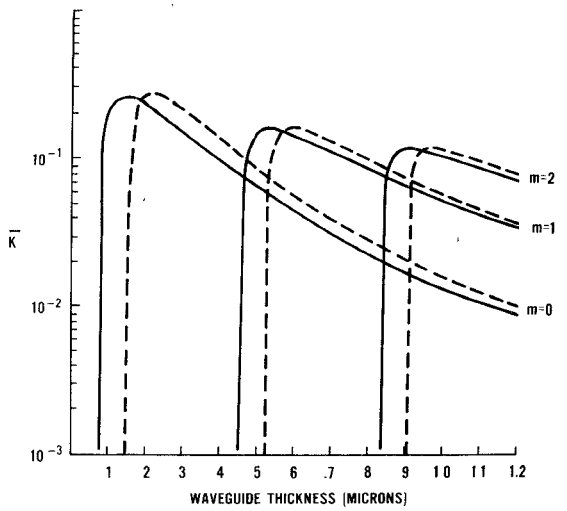

Fig. 13. Normalized coupling constant as a function of waveguide thickness for $n_s = 3.414$, $n_f = 3.59$, $n_c = 1$ (solid curves), and $n_c = 3.294$ (dashed curves), and $\lambda = 0.83$ μm. (From [44].)

This implies the need for very small periods Λ of the order of 1000–2000 Å. These have been used for filters [38] and distributed feedback lasers [41]–[44].

A derivation of the coupling coefficient κ for the corrugated film structure of Fig. 11 is given in [9]. For backward scattering of TE modes it can be written in the form [42]

$$\kappa = \frac{\pi h}{\lambda} \frac{(n_f^2 - N^2)}{2wN} \tag{34}$$

which is accurate to first order in the corrugation height h. N and w are the effective index and the effective guide thickness defined earlier. The dependence of κ on the film thickness f is shown in Fig. 13, which is taken from [44] and applies to a GaAlAs waveguide at $\lambda = 8300$ Å with $n_f = 3.59$, and $n_s = 3.414$. The scale of the normalized quantity $\bar{\kappa} = \lambda\kappa/\pi h$ is used for the ordinate. Results are shown for the three lowest order modes ($m = 0,1,2$). The solid lines refer to a cover index of $n_c = 1$ (air) and the dashed curves refer to an $n_c = 3.294$ ($Al_{0.5}Ga_{0.5}As$). We note that the maximum value for κ occurs fairly close to cutoff, and that a change in the value of n_c has relatively little influence on this value.

D. Coupling to Radiation Modes

When we choose a grating vector K for a periodic waveguide such that

$$\beta = K + n_s k \sin \Theta \tag{35}$$

then we couple a guided mode to a radiation mode. This results in light leaking from the guide into the substrate at an angle Θ with respect to the film normal. We have drawn the wave vector diagram for this case in Fig. 14, where the circle is the locus of all wave vectors allowed in the substrate. Due to the leakage the guided wave amplitude R decreases exponentially with distance

$$R(z) = R_0 \exp(-z/l) \tag{36}$$

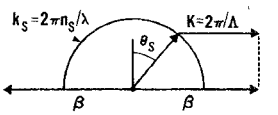

Fig. 14. Wave vector diagram indicating the grating coupling of a guided mode (β) to a radiation mode by a periodicity in the waveguide (K).

where l is called the leakage length. Coupling to radiation modes is the mechanism by which waveguide inhomogeneities can cause scattering losses [8], [9], and it is also the basis for the grating couplers [45], [46] which can feed laser beams into guided film modes.

IV. FABRICATION TECHNIQUES

The past few years have seen the exploration of a great variety of techniques for the fabrication of guiding films with low loss, the precise delineation of circuit and device patterns, and for the machining of these patterns with high resolution. The following examples were selected to illustrate this variety.

A. Film Fabrication

To form a planar slab guide we need to fabricate a uniform layer of higher index on a planar substrate. One of the earlier methods to achieve this employed ion exchange in glass [47]. A recent workhorse for the fabrication of devices has been a film of Corning 7059 glass produced by RF sputtering on microscope slides [48]. This technique yields single mode guides with losses below 1 dB/cm and indices of about $n_f = 1.62$ and $n_s = 1.52$. The use of ion implantation is in its early stages of exploration. Waveguides have been made by implanting Li in fused silica [49] and protons in GaP [50] and GaAs [51] substrates.

Solid-state diffusion is another promising technique which can also be used to form waveguides in crystal substrates. Naturally the result is a guide with a graded refractive index profile. Waveguides have been made by diffusion of Se into CdS crystals [52], of Cd and Se into ZnS [53], and of Cd into ZnSe [53] substrates. Outdiffusion [54] of Li has been used to produce waveguides in $LiNbO_3$ and $LiTaO_3$, both modulator materials of great interest. The confinement obtainable with these guides is limited to about 12 μm. Recently, two promising techniques have been reported which can produce low-loss single-mode waveguide layers as thin as 1 μm. These employ the diffusion of Nb into $LiTaO^3$ [55], and the diffusion of Ti into $LiNbO_3$ [56]. Interesting because of their high index are films of Ta_2O_5 prepared by oxidizing a sputtered Ta film [57].

The epitaxial growth of single-crystal films has become a key element in the production of electrooptic, magnetooptic, or laser-active guiding layers. To achieve the required higher index these layers are usually of a different material composition than the substrate and the matching of lattice constants becomes an important consideration. The epitaxial GaAlSs heterostructure layers made for

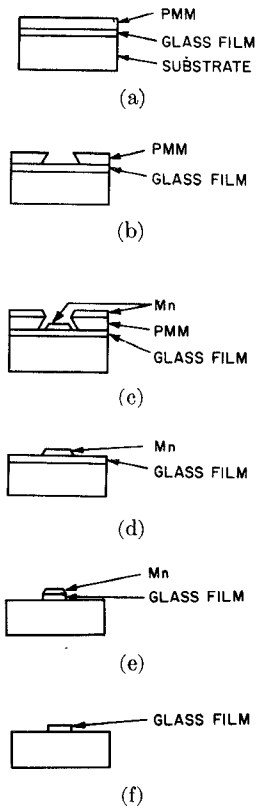

Fig. 15. Typical sequency for fabricating strip guide patterns. (From [72].)

junction lasers [58]–[60] are a prime example for the use of this method. Other examples are the electrooptic epitaxial ZnO layers on sapphire [61], the epitaxial ADP-KDP mixed-crystal films on KDP substrates [62], and the epitaxial layers of $LiNbO_3$ grown on $LiTaO_3$ substrates [63], [64]. Epitaxial magnetooptic waveguides have been prepared in a variety of garnets [65] which are relatives of the magnetic bubble materials.

The exploration of organic films as waveguides has included the use of epoxy films [66], [67], of organosilicon films [68] showing extremely low losses, and of layers of photoresist [69], [70] or electron resist [71].

B. Circuit Patterns by Scanning Electron Microscopy

Strip guides and more complicated integrated optics circuit and device structures are made by a planar technology which is very similar to the electronic integrated circuit technology and to that used for surface acoustic wave devices. Fig. 15 illustrates a typical fabrication sequence [72] for a strip guide. In the first step (a) one starts with a planar slab guide (glass) on which one spin-coats a suitable photoresist or electronresist layer (polymethyl methacrylate). The resist is exposed to an image of the device pattern which is produced optically or by a scanning electron beam. After development, the resist masks the film areas to be etched later (b). In the third step one deposits a metal layer (Mn) over mask and film (c). Subsequently, the resist is removed (with acetone), and one is left with a metal strip masking the film (d). Now the surrounding film material is etched away, e.g., by RF back sputtering, leaving the structure shown in (e). After removal of the metal (with hydrochloric acid), the desired strip guide pattern is obtained.

For integrated optics work we usually require patterns with a high resolution (guide separation of 1 μm are typical) and waveguides with an edge roughness better than 500 Å. Conventional photolithographic techniques are not good enough for this job. Satisfactory results are expected from scanning electron beam techniques. These are being explored by several groups and some devices have already been fabricated that way [71]–[74].

When we think about the economics of scanning electron beam techniques we should recall that high-resolution pattern replication techniques are under development for the mass fabrication of electronic integrated circuits. In one example [75], soft X-rays are employed to reuse a mask with submicrometer resolution many times. In another technique [76] a master mask is used which, upon exposure to UV, emits electrons in the desired pattern. These techniques are also of interest for integrated optics.

C. Grating Patterns by Laser Interference

The masks for periodic structures of high resolution can be written by a technique borrowed from holography. Here a photoresist layer (e.g., Shippley AZ 1350) is exposed to the interference pattern produced by two coherent laser beams incident at an angle to each other [42], [77], [78]. The angle of incidence and the wavelength of the laser light control the fringe spacing. To achieve ultrafine grating periods ($\Lambda \approx 1000$ Å) the UV line at 3250 Å of the CW helium–cadmium laser has been used.

It appears that the laser-interference technique is more naturally suited to the production of high-resolution gratings than the scanning electron-beam techniques, yielding good uniformity of the grating period with greater ease.

D. High-Resolution Etching Techniques

The previously mentioned sputter etching technique [72] is not the only way to produce strip guides or more complicated patterns. Strip guides have also been made by masked diffusion [52], [53] and by ion implantation through a mask [79], [80]. Other techniques under exploration are the embossing [81] and the photolocking [82] of strip guide patterns written directly with a laser beam. A technique capable of very high resolution is ion-beam etching using photoresist as a mask material [42], [77], [78]. Typically, the etching is done with a beam of argon ions at a few kilovolts, and the substrate remains relatively cool during the process. Fig. 16 shows a surface corrugation on a glass waveguide etched that way to make a filter device [38]. The period shown there is 1900 Å, but the technique is capable of producing corrugations with periods as small as 1000 Å, and corrugation depths of about 500 Å [78], [43].

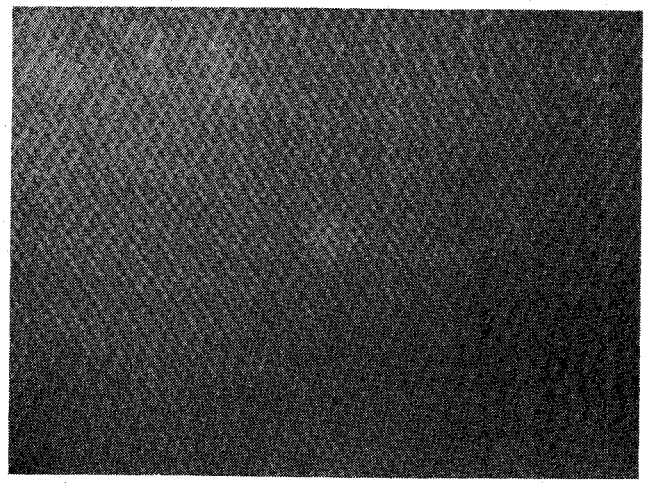

(a)

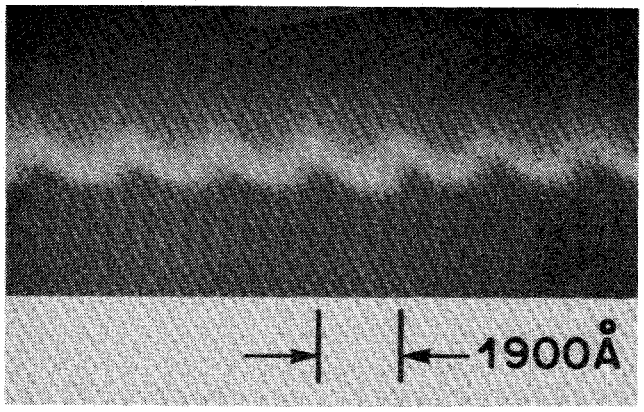

(b)

Fig. 16. Ion beam etched gratings. Scanning electron micrographs of corrugation etched into a glass waveguide. (a) Top view. (b) End view.

V. DEVICES

In the past few years a great variety of devices have been explored experimentally, including directional couplers, filters, modulators, light deflectors, and the application of guided-wave techniques to lasers. In this section we will try to illustrate this work. Because of space limitations, this illustration has to remain quite selective. For more complete and up-to-date reviews the reader should consult the articles in this issue by Kaminow [83] on modulators, and by Panish [84] on GaAs injection lasers.

A. Beam to Film Couplers

Beam-to-film couplers are devices that allow us to feed the light from a laser beam into a film waveguide. Fig. 17 shows two coupler types used in the laboratory, the prism coupler [85], [86] and the grating coupler [45], [46]. In the first method [Fig. 17(a)] a prism of high index n_p

$$n_p \gtrsim n_f \tag{37}$$

is brought close enough to the film guide (typically 1000 Å) so that it can interact with the evanescent field of a guided mode. This makes the structure leaky and coupling is possible. In order to achieve coupling we also have to

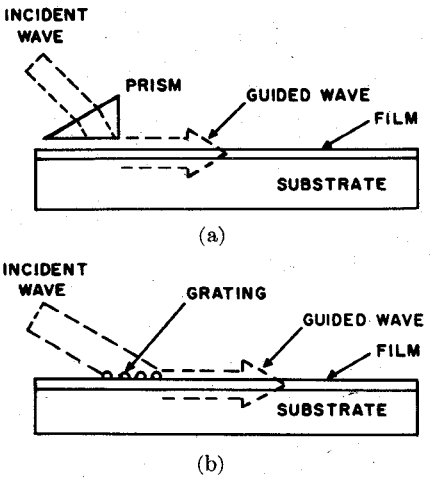

Fig. 17. (a) Schematic of prism coupler. (b) Schematic of grating coupler. (From [5].)

provide synchronism (phase matching) and satisfy

$$\beta = kn_p \sin \Theta_p \tag{38}$$

by choosing the correct injection angle Θ_p in the prism relative to the film normal.

To make a grating coupler [Fig. 17(b)] we introduce a periodicity into the guide, e.g., by depositing a photoresist grating. This will lead to coupling of a guided mode to radiation modes as discussed earlier in Section III.

The overall behavior of prism and grating couplers is rather similar. For uniform coupling, i.e., uniform prism film gaps or uniform grating strength, the theoretically predicted maximum coupling efficiency is about 81 percent for both uniform or Gaussian beam cross section [85]–[89]. This is achieved when the width of w_B of the incident laser beam matches the leakage length l of the coupler [see (36)], i.e., if

$$w_B \approx l. \tag{39}$$

To approach this value with grating couplers, care must be taken that unwanted grating orders are suppressed. This was done in a recently reported coupler [87] using a photoresist grating, reverse coupling [46], and light incident through the substrate. Efficiencies exceeding 70 percent were obtained.

The theoretical coupler efficiencies can approach 100 percent when the coupling is tapered to match the input beam to the leakage field of the guide [88], [89].

A third coupler type is described in [90]. Here the film thickness is tapered down at the edge of the guide resulting in coupling of light into the substrate.

B. Directional Couplers

The directional coupler is a familiar microwave device. The strip-guide version of its integrated optics analogue is shown in Fig. 18, where we have two strip guides approaching each other, running close and parallel over the interaction distance, and then separating again. When the propagation constants of the two guides are matched we

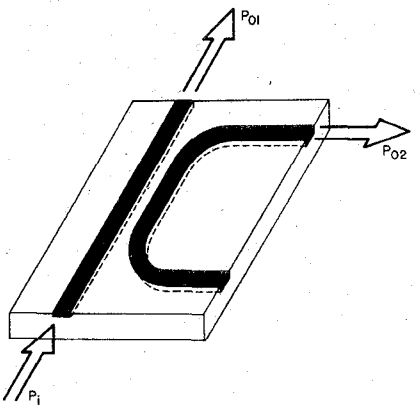

Fig. 18. Sketch of a strip-guide configuration forming an optical directional coupler.

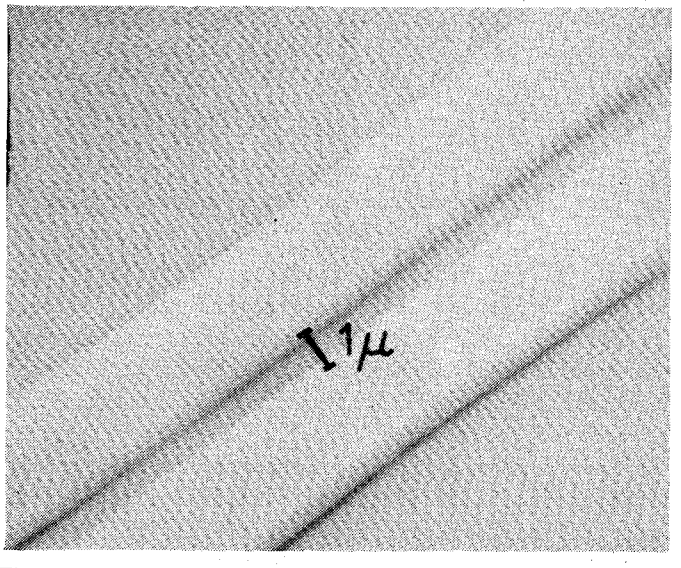

Fig. 19. Scanning electron micrograph of the interaction region of a directional coupler formed by two strip guides. (From [72].)

can get codirectional coupling and exchange of power between the guides. The coupling constant κ (and coupling length) between the parallel guides is determined by their separation c and the decay constant γ_y in the film plane

$$\kappa \propto \exp(-\gamma_y c) \tag{40}$$

where the exponential dependence indicates a great sensitivity of the coupling length to variations in the gap spacing.

In the first experimental work on directional couplers, the exchange and complete transfer of power [see (27)] between parallel strip guides in GaAs has been observed [19], and couplers of the geometry shown in Fig. 18 have been made by scanning electron beam techniques [72], [74]. Fig. 19 shows the smooth edges of the glass guides in the interaction region of the coupler of [72], where the guide spacing c was about 1 μm.

C. Filters

The filter characteristics of periodic waveguides have also been seen experimentally [38], [39]. A periodic guide

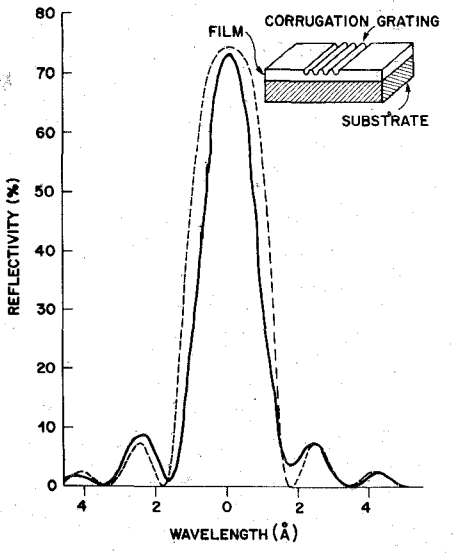

Fig. 20. Frequency response of a corrugated waveguide filter. The dashed curve shows the theoretical prediction. (From [38].)

of length L provides a band rejection filter with a fractional bandwidth of approximately

$$\Delta\lambda/\lambda \approx \Lambda/L \tag{41}$$

centered at the Bragg wavelength $2N\Lambda$ [see (33)].

Fig. 20 shows the filter response of a corrugated glass waveguide at 0.57 μm reported in [38]. The filter was fabricated by means of UV laser exposure and ion-beam etching. It was $L = 0.57$ mm long, and had corrugations with a period of about $\Lambda = 2000$ Å and a depth of 460 Å. The response was measured with a tunable dye laser showing a bandwidth of 4 Å and good agreement with the theory of contradirectional coupling.

In recent experiments [91] filter bandwidths as low as 0.1 Å were obtained. This requires longer filter lengths and careful attention to tolerances imposed on the film thickness. The achieved bandwidth indicates that the fabricated grating period Λ had deviations from uniformity smaller than 10^{-5} over the length of the filter.

D. Modulators

Guided-wave modulators are, perhaps, the integrated optics devices which have developed most rapidly in the recent past. Here, apart from compactness and stability, the guided-wave approach promises low drive powers and low drive voltages. The reason for this is that no diffraction spreading occurs and the light can be contained within long structures having small cross sections with diameters of the order of a wavelength. However, when one contemplates the use of these modulators as separate devices, one should bear in mind two potential drawbacks. One is the need for coupling to such a device, and the other is a possible limitation in the guided optical power to prevent damage or breakdown due to the high power densities associated with small guide cross sections.

Several modulation effects and device structures have been explored and [83] gives a detailed review. We will

mention here electrooptic, magnetooptic, and electroabsorption modulators. An important measure of device performance is the drive power dissipated per unit bandwidth of the signal for a given modulation index. Others are the drive voltage, the speed, and the optical insertion loss. If the light is confined in a strip guide with an effective guide cross section $w_x \cdot w_y$ and length L then we have a drive power P per bandwidth $\Delta\nu$ which is proportional to

$$P/\Delta\nu \propto w_x w_y / L. \tag{42}$$

Here we have assumed that the applied modulating field is confined to the same volume as that occupied by the light. This means that an electrode configuration is required that matches the applied field distribution to that of the guided light.

Electrooptic modulators use materials in which a change of the refractive index can be induced by an applied electric field. This results in a phase modulation of the light passing through. Promising electrooptic materials are $LiNbO_3$ and $LiTaO_3$ which are transparent for wavelengths from 0.4 to 4 μm. Outdiffused waveguides in $LiNbO_3$ have been used to make high-speed guided-wave phase modulators [92], [93]. Fig. 21 shows a sketch of a recent device [93] where a ridge guide is employed to confine the light within the film plane as well. The electrodes were evaporated along the ridge which is about 20 μm wide. This modulator requires a drive voltage of 1.2 V to produce a phase modulation of 1 rad and uses a power of 20 μW/MHz of bandwidth. The method of diffraction by electrooptically induced gratings has been proposed to obtain amplitude modulation of the light [94] and modulators in ZnO waveguides have been constructed that way [95]. Fig. 22 shows the electrode structure used to induce such a grating in a thin $LiNbO_3$ crystal [96]. Grating modulation has also been reported with the new Nb-indiffused waveguides in $LiTaO_3$ [55]. Amplitude modulation can also be achieved with only two electrodes if one uses the induced prism effect due to the inhomogeneity of the applied field. This was demonstrated in work on Schottky-barrier GaAs modulators operating at 10.6 μm [97].

Electrooptic effects are also obtained in the depletion layer of reverse-biased semiconductor diodes which can also serve as a waveguide. Such guided-wave modulators have been made using the p-n junctions in GaP [98] and Schottky barriers in GaAs [99]. Recently, a GaAlAs double heterostructure was used to construct a modulator requiring 10 V and 0.1 mW/MHz of bandwidth for phase modulation of 1 rad at 1.15 μm [100]. This device has a potential bandwidth of 4 GHz.

In magnetooptic modulators one uses the Faraday rotation to achieve mode conversion and, thereby, amplitude modulation. Guided-wave modulators of this type have been built with epitaxial films of iron garnets [35]. They have operated at frequencies up to 80 MHz at a wavelength of 1.15 μm. These devices are very sensitive and require applied magnetic fields of only 1/100 Oe to switch the output light on or off.

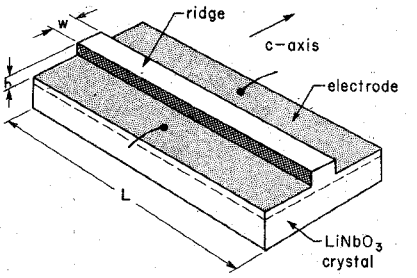

Fig. 21. Sketch of $LiNbO_3$ phase modulator with a ridge guide on an outdiffused waveguide layer. (From [93].)

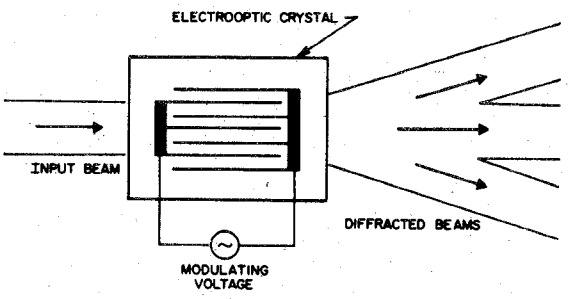

Fig. 22. Interdigital electrode structure used to induce an electrooptic grating. (From [96].)

Electroabsorption, or the Franz–Keldysh effect, is another way to achieve direct amplitude modulation. These devices use an electric-field induced shift of the band edge (and, therefore, operate near the band edge). An electroabsorption modulator operating at 0.9 μm was reported in [101]. It uses GaAlAs waveguides and requires 0.2 mW/MHz for an amplitude modulation of 90 percent.

E. Light Deflectors

The technology of bulk acoustooptic devices for the deflection and modulation of light is already fairly well developed. In the integrated optics analogues of these devices guided optical waves are scattered from surface acoustic waves [14]. This approach allows a close confinement and overlap of the optical and acoustical fields resulting in a reduction of the required acoustic drive power. The surface acoustooptic interaction is similar to the scattering of light sketched in Fig. 22 with the difference that the gratings are induced acoustooptically. The figure shows Raman–Nath scattering with several diffracted orders as it may be used for modulators. For deflectors one uses a codirectional coupled wave interaction with light incident at the Bragg angle and only one significant diffracted order.

In order to launch the surface waves we need surface-acoustic transducers. Comparing these to bulk transducers we find that, at present, it is more difficult to obtain good efficiencies over large bandwidth, but there are also advantages: surface-wave transducers can be fabricated with a planar technology, and complicated electrode patterns for steering the acoustic column can be made with relative ease [102]. Such a pattern is sketched in Fig. 23(b) while Fig. 23(a) shows the hard-to-fabricate

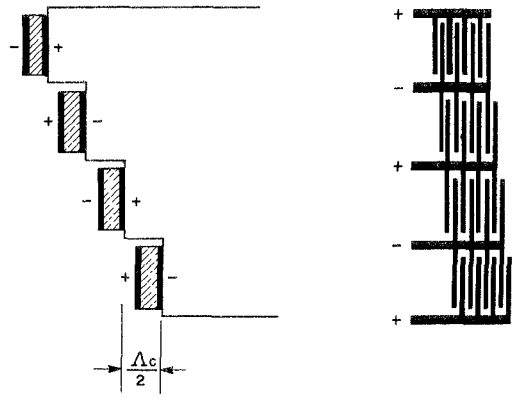

Fig. 23. Sketch of phased arrays of acoustic bulk (a) and surface-wave (b) transducers.

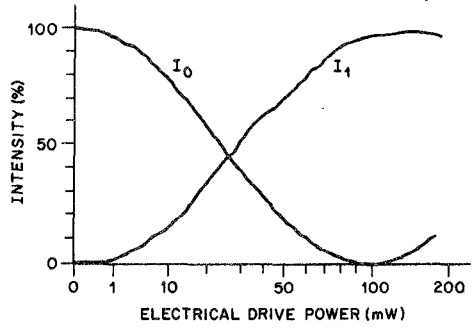

Fig. 24. Deflected (I_1) and transmitted (I_0) light intensity as a function of acoustic drive power for a thin-film light deflector using titanium-diffused waveguides on $LiNbO_3$. (From [105].)

stepped surface required for a comparable transducer array for bulk waves.

Recently, optical guides have been fabricated on materials such as $LiNbO_3$ which have a better acoustooptic figure of merit than the materials used for earlier devices (e.g., quartz). Experiments with light deflectors have been made with As_2Se_3 guides [103] on $LiNbO_3$, with out-diffused $LiNbO_3$ guides [104] and with titanium-diffused guides [105] on $LiNbO_3$. Fig. 24 shows the results achieved with the recent titanium-diffused waveguides at an acoustic frequency of 170 MHz [105]. The Bragg diffracted light intensity I_1 is shown as a function of acoustic power; about 8 mW are needed to diffract 70 percent of the incident light over a bandwidth of 30 MHz of the acoustic frequency. Note also that the measured data agree well with the coupled-wave behavior predicted by (27). We should recall here that $LiNbO_3$ is not the ultimate in acoustooptics and still better materials exist. An example is paratellurite (TeO_2) which has been used for high-performance light deflectors in bulk form [106]. No optical waveguides on these materials are available as yet. Experimental studies were made of a variety of other acousto-optic interaction geometries different from those described above. These include the inducing of a grating by launching acoustic shear waves normal to the film guide [107], and the scattering of light from the guide into the substrate induced by a surface-acoustic wave [108] which acts like a grating coupler.

F. Lasers

Along with the promise of small size, compactness, and compatibility with other waveguide devices, the application of guided-wave techniques to lasers promises stability of output, low threshold, low power consumption, and low heat dissipation. The techniques under exploration include the confinement of the light to a thin film, the use of structures such as stripe contacts or ridge guides for confinement in the film plane and for transverse mode control, and the use of periodic structures to provide (distributed) feedback, control of the longitudinal modes, and a narrow output spectrum. Guided-wave techniques are in various phases of their development for semiconductor lasers, solid-state lasers, gas lasers, and organic dye lasers. While the use of guiding films in semiconductor lasers is almost as old as the semiconductor laser itself, the use of waveguides in dye lasers has, so far, been confined to the laboratory for the purpose of exploring new guided-wave structures. For thin-film solid-state lasers, optical pumping with light-emitting diodes or other lasers has been considered [109]. Here problems of pump inefficiencies and the associated lower overall efficiency have to be overcome. The present standard of comparison for these devices are the electrically pumped semiconductor lasers which can offer relatively high efficiencies.

Recently, $Al_xGa_{1-x}As$ heterostructure junction lasers have become available which are capable of long-lived CW operation at room temperature. These devices are of great interest for optical communications. For a detailed review of these lasers we refer the reader to [84], [110], [111], or [112]. The refractive index of the $Al_xGa_{1-x}As$ material decreases with the Al concentration x following very nearly the rule

$$n(x) = n(o) - 0.45x. \tag{43}$$

A heterostructure waveguide can thus be formed by sandwiching an epitaxial layer of GaAs with lower index $Al_xGa_{1-x}As$ material. A typical concentration value is $x = 0.3$. While heteroepitaxy is now the standard for junction lasers, the exploration of other fabrication techniques is being continued. An example is the recent production of junction lasers formed by implantation of Zn^+ ions in n-type GaAs doped with tellurium [113]. Pulsed lasers operation of these devices was observed at low temperatures (77K).

For the optically pumped thin-film solid-state lasers a high concentration of active ions is preferred. Concentration quenching of the fluorescence, however, calls for compromise solutions [109]. Initial attempts with thin-film solid-state lasers have already shown some success. Lasers with Ho^{3+} doped aluminum garnet films [114] have operated at 2.1 μm, and lasers with similar films doped with Nd^{3+} have operated at 1.06 μm [115]. Both film types were epitaxially grown on YAG substrates. Relatively large index differences were achieved with Nd^{3+} doped

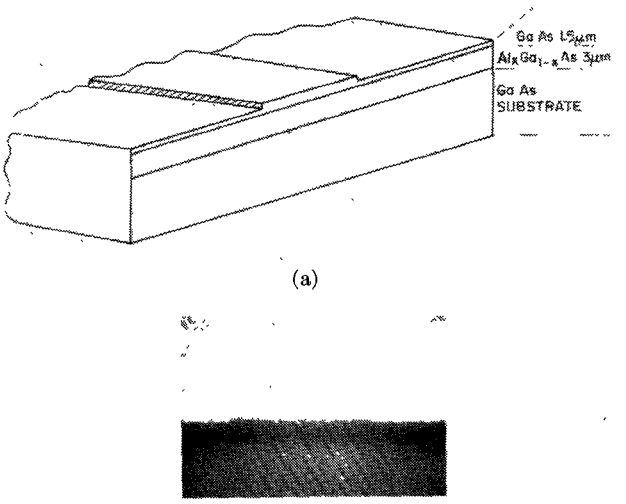

(a)

(b)

Fig. 25. Sketch (a) and scanning electron micrograph (b) of a GaAs ridge guide. (From [118].)

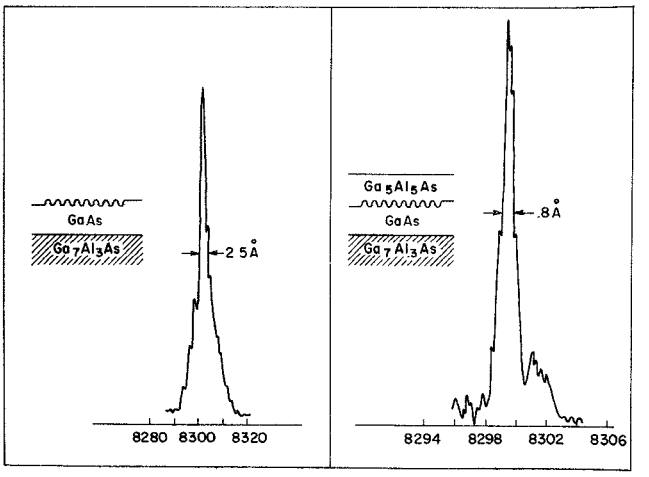

(a) (b)

Fig. 26. Output spectra of optically pumped AlGaAs lasers with periodic heterostructures. In case (a) the cover material was air, and in case (b) regrown AlGaAs. (From [44].)

epitaxial films of YAG ($n_f = 1.818$) and $CaWO_4$ ($n_f = 1.89$) grown on sapphire ($n_s = 1.77$) substrates [116]. Thin-film lasers have also been made of $CdS_{1-x}Se_x$ layers grown on CdS substrates [117].

GaAs junction lasers with a stripe geometry have been developed to provide lasers operating in a stable and pure transverse mode [112]. Stripe contacts and mesa stripes are two key examples for stripe-geometry structures. These structures usually confine both the light and the charge carriers. In principle, separated optical confinement can be achieved by the use of strip waveguides such as those discussed in Section II-C. Recently, ridge waveguides have been investigated for this purpose [118], and confinement of light and pure modes were observed in passive structures. The ridges were formed by anodization etching of GaAs films on $Al_xGa_{1-x}As$ substrates. Fig. 25 shows such a ridge guide with a width of approximately 10 μm and a film thickness of about 0.8 μm.

Distributed feedback structures promise to provide compact low-loss optical cavities for thin-film lasers which allow longitudinal mode control and frequency selection. Essentially, these are periodic waveguide structures superimposed on the gain medium. The feedback mechanism is backward Bragg scattering. While the first studies of the distributed feedback mechanism were done with dye lasers, the recent work has focused on the materials and fabrication problems of providing distributed feedback for AlGaAs lasers [43], [44], [119], [120]. Here the structures of interest take the form of a surface corrugation of the GaAs layer, as indicated in Fig. 26. Problems under study include the fabrication of the ultrafine grating-like structure where periods of about 1000 Å are needed, and the regrowing of AlGaAs crystal layers upon the corrugated GaAs [44], [119], [120]. Fig. 26 shows the narrowing of the linewidth achieved with the periodic heterostructure lasers of [44], where the corrugation was fabricated by UV-laser exposure and ion-beam etching techniques and regrowth was accomplished with a dummy-seed-crystal technique preventing back-dissolving of the corrugation. These lasers were pumped optically with a pulsed dye laser and output spectra less than 1 Å in width were observed at 77K. Very recently [120], distributed feedback operation was demonstrated in electrically pumped single-heterojunction GaAs lasers at low temperatures (77K). Here corrugations were used which were etched 1300 Å deep and had a period of 3500 Å designed to utilize third-order scattering.

VI. CONCLUSIONS

We have tried to collect here the chief principles, underlying thoughts and promises of the field of integrated optics, and to illustrate recent experimental work on guided-wave devices. Whereas the field is still in its infancy it has attracted considerable interest and stimulated an extensive exploratory effort. This is reflected in the over 100 references we have cited, and these are only a fraction of the literature that is already available. Indeed, since this paper was written there have appeared two additional papers reviewing integrated optics [121], [122]. Integrated optics has drawn on many other disciplines including microwave theory and techniques, integrated circuit technology, solid-state physics, and optics and new devices, materials, and fabrication techniques have emerged. The field is now in a state of great flux and there are still many problems awaiting a solution, a main problem being the lack of a simple and efficient method of coupling optical fibers to thin-film or strip-guide devices.

REFERENCES

[1] S. E. Miller, "Integrated optics: An introduction," *Bell Syst. Tech. J.*, vol. 48, p. 2059, Sept. 1969.
[2] J. E. Goell, R. D. Standley, and T. Li, *Electronics*, vol. 20, pp. 60–67, Aug. 1970.
[3] J. E. Goell and R. D. Standley, "Integrated optical circuits," *Proc. IEEE (Special Issue on Optical Communications)*, vol. 58, pp. 1504–1512, Oct. 1970.
[4] P. K. Tien, "Light waves in thin films and integrated optics," *Appl. Opt.*, vol. 10, p. 2395, Nov. 1971.
[5] S. E. Miller, "A survey of integrated optics," *IEEE J. Quantum*

Electron. (Special Issue on 1971 IEEE/OSA Conference on Laser Engineering and Application, Part II of Two Parts), vol. QE-8, pp. 199–205, Feb. 1972.
[6] S. E. Miller, E. A. J. Marcatili, and T. Li, "Research toward optical-fiber transmission systems (*Invited Paper*)," *Proc. IEEE*, vol. 61, pp. 1703–1753, Dec. 1973.
[7] N. S. Kapany and J. J. Burke, *Optical Waveguides*. New York: Academic, 1972.
[8] D. Marcuse, *Light Transmission Optics*. New York: Van Nostrand Reinhold, 1972.
[9] ——, Theory of Dielectric Optical Waveguides. New York: Academic, 1974.
[10] E. A. J. Marcatili, *Bell Syst. Tech. J.*, vol. 48, p. 2071, Sept. 1969.
[11] H. Kogelnik and V. Ramaswamy, *Appl. Opt.*, vol. 13, pp. 1857–1862, Aug. 1974.
[12] J. J. Burke, *Opt. Sci. Newsletter (Univ. Arizona)*, vol. 5, p. 31, 1971; also, *Opt. Sci. Newsletter (Univ. Arizona)*, vol. 5, p. 6, 1971.
[13] H. Kogelnik and H. P. Weber, *J. Opt. Soc. Amer.*, vol. 64, pp. 174–185, Feb. 1974.
[14] L. Kuhn, M. L. Dakss, P. F. Heidrich, and B. A. Scott, *Appl. Phys. Lett.*, vol. 17, p. 265, Sept. 1970.
[15] R. Shubert and J. H. Harris, "Optical surface waves on thin films and their application to integrated data processors," *IEEE Trans. Microwave Theory Tech. (1968 Symposium Issue)*, vol. MTT-16, pp. 1048–1054, Dec. 1968.
[16] R. Ulrich and R. J. Martin, *Appl. Opt.*, vol. 10, p. 2077, Sept. 1971.
[17] F. Zernike, *Appl. Phys. Lett.*, vol. 24, p. 285, Mar. 1974.
[18] P. Kaiser, E. A. J. Marcatili, and S. E. Miller, *Bell Syst. Tech. J.*, vol. 52, p. 265, 1973.
[19] S. Somekh *et al.*, *Appl. Opt.*, vol. 13, p. 327, Feb. 1974.
[20] J. E. Goell, *Appl. Opt.*, vol. 12, p. 2797, Dec. 1973.
[21] H. Furuta, H. Noda, and A. Ihaya, *Appl. Opt.*, vol. 13, p. 322, Feb. 1974.
[22] V. Ramaswamy, *Bell Syst. Tech. J.*, vol. 4, p. 697, Apr. 1974.
[23] W. Schlosser and H. G. Unger, in *Advances in Microwaves*. New York: Academic, 1966, p. 319.
[24] J. E. Goell, *Bell Syst. Tech. J.*, vol. 48, p. 2133, Sept. 1969.
[25] E. A. J. Marcatili, *Bell Syst. Tech. J.*, vol. 4, p. 645, Apr. 1974.
[26] W. H. Zachariasen, *Theory of X-Ray Diffraction in Crystals*. New York: Wiley, 1945.
[27] C. F. Quate, C. D. Wilkinson, and D. K. Winslow, "Interaction of light and microwave sound," *Proc. IEEE (Special Issue on Ultrasonics)*, vol. 53, pp. 1604–1623, Oct. 1965.
[28] H. Kogelnik, *Bell Syst. Tech. J.*, vol. 48, p. 2909, Nov. 1969.
[29] S. E. Miller, *Bell Syst. Tech. J.*, vol. 33, p. 661, May 1954.
[30] J. R. Pierce, *J. Appl. Phys.*, vol. 25, p. 179, Feb. 1954.
[31] W. H. Louisell, *Coupled Mode and Parametric Electronics*. New York: Wiley, 1960.
[32] A. Yariv, "Coupled-mode theory for guided-wave optics," *IEEE J. Quantum Electron.*, vol. QE-9, pp. 919–934, Sept. 1973.
[33] S. Wang, M. L. Shah, and J. D. Crow, *Appl. Phys. Lett.*, vol. 19, p. 187, 1971.
[34] T. P. Sosnowski and H. P. Weber, *Opt. Commun.*, vol. 7, p. 47, Jan. 1973.
[35] P. K. Tien *et al.*, *Appl. Phys. Lett.*, vol. 21, p. 394, Oct. 1972.
[36] H. Kogelnik and C. V. Shank, *J. Appl. Phys.*, vol. 43, p. 2327, May 1972.
[37] A. W. Snyder, *J. Opt. Soc. Amer.*, vol. 62, p. 1267, Nov. 1972.
[38] D. C. Flanders, H. Kogelnik, R. V. Schmidt, and C. V. Shank, *Appl. Phys. Lett.*, vol. 24, p. 194, Feb. 1974.
[39] F. W. Dabby, M. A. Saifi, and A. Kestenbaum, *Appl. Phys. Lett.*, vol. 22, p. 190, Feb. 1973.
[40] L. Kuhn, P. F. Heidrich, and E. G. Lean, *Appl. Phys. Lett.*, vol. 19, p. 428, Nov. 1971.
[41] H. Kogelnik and C. V. Shank, *Appl. Phys. Lett.*, vol. 18, p. 152, Feb. 1971.
[42] D. P. Schinke, R. G. Smith, E. G. Spencer, and M. F. Galvin, *Appl. Phys. Lett.*, vol. 21, p. 494, Nov. 1972.
[43] H. W. Yen *et al.*, *Opt. Commun.*, vol. 9, p. 35, Sept. 1973.
[44] C. V. Shank, R. V. Schmidt, and B. I. Miller, *Appl. Phys. Lett.*, vol. 25, pp. 200–201, Aug. 1974.
[45] M. L. Dakss, L. Kuhn, P. F. Heidrich, and B. A. Scott, *Appl. Phys. Lett.*, vol. 16, p. 523, June 1970.
[46] H. Kogelnik and T. P. Sosnowski, *Bell Syst. Tech. J.*, vol. 49, p. 1602, Sept. 1970.
[47] H. Osterberg and L. W. Smith, *J. Opt. Soc. Amer.*, vol. 58, p. 1078, Sept. 1964.
[48] J. E. Goell and R. D. Standley, *Bell Syst. Tech. J.*, vol. 48, p. 3445, Dec. 1969.
[49] R. D. Standley, W. M. Gibson, and J. W. Rodgers, *Appl. Opt.*, vol. 11, p. 1313, 1972.
[50] M. K. Barnoski, R. G. Hunsperger, R. G. Wilson, and G. Tangonan, *J. Appl. Phys.*, vol. 44, p. 1925, 1973.
[51] E. Garmire, H. Stoll, A. Yariv, and R. G. Hunsperger, *Appl. Phys. Lett.*, vol. 21, p. 87, 1972.
[52] H. F. Taylor, W. E. Martin, D. B. Hall, and V. N. Smiley, *Appl. Phys. Lett.*, vol. 21, p. 95, Aug. 1972.
[53] W. E. Martin and D. B. Hall, *Appl. Phys. Lett.*, vol. 21, p. 325, Oct. 1972.
[54] I. P. Kaminow and J. R. Carruthers, *Appl. Phys. Lett.*, vol. 22, p. 326, Apr. 1973.
[55] J. M. Hammer and W. Phillips, *Appl. Phys. Lett.*, vol. 24, p. 545, June 1974.
[56] R. V. Schmidt and I. P. Kaminow, *Appl. Phys. Lett.*, vol. 25, pp. 458–460, Oct. 1974.
[57] D. H. Hensler, J. D. Cuthbert, R. J. Martin, and P. K. Tien, *Appl. Opt.*, vol. 10, p. 1037, May 1971.
[58] Z. I. Alferov *et al.*, *Sov. Phys.—Semicond.*, vol. 2, p. 1289, Apr. 1969.
[59] I. Hayashi, M. B. Panish, and P. W. Foy, "Low-threshold room-temperature injection laser," *IEEE J. Quantum Electron* (Corresp.), vol. QE-5, pp. 211–212, Apr. 1969.
[60] H. Kressel and H. Nelson, *RCA Rev.*, vol. 30, p. 106, Mar. 1969.
[61] J. M. Hammer, D. J. Channin, M. T. Duffy, and J. P. Wittke, *Appl. Phys. Lett.*, vol. 21, p. 358, Oct. 1972.
[62] V. Ramaswamy, *Appl. Phys. Lett.*, vol. 21, p. 183, Sept. 1972.
[63] S. Miyazawa, *Appl. Phys. Lett.*, vol. 23, p. 198, 1973.
[64] P. K. Tien *et al.*, *Appl. Phys. Lett.*, vol. 24, p. 503, May 1974.
[65] ——, *Appl. Phys. Lett.*, vol. 21, p. 207, Sept. 1972.
[66] J. H. Harris, R. Shubert, and J. N. Polky, *J. Opt. Soc. Amer.*, vol. 60, p. 1007, Aug. 1970.
[67] R. Ulrich and H. P. Weber, *Appl. Opt.*, vol. 11, p. 428, Feb. 1972.
[68] P. K. Tien, G. Smolinsky, and R. J. Martin, *Appl. Opt.*, vol. 11, p. 637, Mar. 1972.
[69] D. B. Ostrowsky and A. Jacques, *Appl. Phys. Lett.*, vol. 18, p. 556, June 1971.
[70] H. W. Weber, R. Ulrich, E. A. Chandross, and W. J. Tomlinson, *Appl. Phys. Lett.*, vol. 20, p. 143, Feb. 1972.
[71] J. C. Dubois, M. Gazard, and D. B. Ostrowsky, *Opt. Commun.*, vol. 7, p. 237, Mar. 1973.
[72] J. E. Goell, *Appl. Opt.*, vol. 12, p. 729, Apr. 1973.
[73] J. J. Turner *et al.*, *Appl. Phys. Lett.*, vol. 23, p. 333, Sept. 1973.
[74] D. B. Ostrowsky, M. Papuchon, A. M. Roy, and J. Trotel, *Appl. Opt.*, vol. 13, p. 636, Mar. 1974.
[75] D. L. Spears and H. I. Smith, *Electron. Lett.*, vol. 8, p. 102, Feb. 1972.
[76] B. Fay, D. B. Ostrowsky, A. M. Roy, and J. Trotel, *Opt. Commun.*, vol. 9, p. 424, Dec. 1973.
[77] H. L. Garvin *et al.*, *Appl. Opt.*, vol. 12, p. 455, Mar. 1973.
[78] C. V. Shank and R. V. Schmidt, *Appl. Phys. Lett.*, vol. 23, p. 154, Aug. 1973.
[79] J. E. Goell, R. D. Standley, W. M. Gibson, and J. W. Rodgers, *Appl. Phys. Lett.*, vol. 21, p. 72, July 1972.
[80] S. Somekh *et al.*, *Appl. Phys. Lett.*, vol. 22, p. 46, Jan. 1973.
[81] R. Ulrich *et al.*, *Appl. Phys. Lett.*, vol. 20, p. 213, Mar. 1972.
[82] E. A. Chandross, C. A. Pryde, W. J. Tomlinson, and H. P. Weber, *Appl. Phys. Lett.*, vol. 24, p. 72, Jan. 1974.
[83] I. P. Kaminow, "Optical waveguide modulators," this issue, pp. 57–70.
[84] M. B. Panish, "Heterostructure injection lasers," this issue, pp. 20–30.
[85] P. K. Tien, R. Ulrich, and R. J. Martin, *Appl. Phys. Lett.*, vol. 14, p. 291, May 1969.
[86] J. H. Harris and R. Shubert, in *International Scientific Radio Union Spring Meeting Conf. Abstracts*, Apr. 1969, p. 71.
[87] D. Dalgoutte, *Opt. Commun.*, vol. 8, p. 124, June 1973.
[88] R. Ulrich, *J. Opt. Soc. Amer.*, vol. 61, p. 1467, Nov. 1971.
[89] J. H. Harris and R. Shubert, "Variable tunneling excitation of optical surface waves," *IEEE Trans. Microwave Theory Tech.*, vol. MTT-19, pp. 269–276, Mar. 1971.
[90] P. K. Tien and R. J. Martin, *Appl. Phys. Lett.*, vol. 18, p. 398, May 1971.
[91] R. V. Schmidt, D. C. Flanders, C. V. Shank, and R. D. Standley, *Appl. Phys. Lett.*, vol. 25, p. 651, Dec. 1974.
[92] I. P. Kaminow, J. R. Carruthers, E. H. Turner, and L. W. Stulz, *Appl. Phys. Lett.*, vol. 22, p. 540, May 1973.
[93] I. P. Kaminow, V. Ramaswamy, R. V. Schmidt, and E. H. Turner, *Appl. Phys. Lett.*, vol. 24, p. 622, June 1974.
[94] J. F. S. Ledger and E. A. Ash, *Electron. Lett.*, vol. 4, p. 99, Mar. 1968.
[95] J. M. Hammer, D. J. Channin, and M. T. Duffy, *Appl. Phys. Lett.*, vol. 23, p. 176, Aug. 1973.
[96] M. A. deBarros and M. G. Wilson, *Proc. Inst. Elec. Eng.*, vol. 119, p. 807, July 1972.
[97] P. K. Cheo, *Appl. Phys. Lett.*, vol. 22, p. 241, Mar. 1971.
[98] F. K. Reinhart, *J. Appl. Phys.*, vol. 39, p. 3426, June 1968.
[99] D. Hall, A. Yariv, and E. Garmire, *Opt. Commun.*, vol. 1, p. 403, Apr. 1970.

[100] F. K. Reinhart and B. I. Miller, *Appl. Phys. Lett.*, vol. 20, p. 36, Jan. 1972.
[101] F. K. Reinhart, *Appl. Phys. Lett.*, vol. 22, p. 372, Apr. 1973.
[102] R. M. De La Rue, C. Stewart, C. D. Wilkinson, and I. R. Williamson, *Electron. Lett.*, vol. 9, p. 326, July 1973.
[103] Y. Omachi, *J. Appl. Phys.*, vol. 44, p. 3928, Sept. 1973.
[104] R. V. Schmidt, I. P. Kaminow, and J. R. Carruthers, *Appl. Phys. Lett.*, vol. 23, p. 417, Oct. 1973.
[105] R. V. Schmidt and I. P. Kaminow, *IEEE J. Quantum Electron.* (Corresp.), vol. QE-11, pp. 57–59, Jan. 1975.
[106] A. W. Warner, D. L. White, and W. A. Bonner, *J. Appl. Phys.*, vol. 43, p. 4489, Nov. 1972.
[107] M. L. Shah, *Appl. Phys. Lett.*, vol. 23, p. 75, July 1973.
[108] F. R. Gfeller and C. W. Pitt, *Electron. Lett.*, vol. 8, p. 549, Nov. 1972.
[109] J. P. Wittke, *RCA Rev.*, vol. 33, p. 674, Dec. 1972.
[110] M. P. Panish and I. Hayashi, *Applied Solid State Science*. New York: Academic, 1974.
[111] H. Kressel, in *Lasers*, A. K. Levine and A. deMaria, Ed. New York: Dekker, 1971.
[112] L. A. D'Asaro, *J. Luminescence*, vol. 7, pp. 310–337, 1973.
[113] M. K. Barnoski, R. G. Hunsperger, and A. Lee, *Appl. Phys. Lett.*, vol. 24, pp. 627–628, June 1974.
[114] J. P. van der Ziel, W. A. Bonner, L. Kopf, and L. G. Van Uitert, *Phys. Lett.*, vol. 42A, p. 105, 1972.
[115] J. P. van der Ziel *et al.*, *Appl. Phys. Lett.*, vol. 22, p. 656, June 1973.
[116] J. G. Grabmaier *et al.*, *Phys. Lett.*, vol. 43A, p. 219, Mar. 1973.
[117] M. Kawabe, H. Kotani, K. Masuda, and S. Namba, to be published.
[118] F. K. Reinhart, R. A. Logan, and T. P. Lee, *Appl. Phys. Lett.*, vol. 24, p. 270, Mar. 1974.
[119] M. Nakamura *et al.*, *Appl. Phys. Lett.*, vol. 24, p. 466, May 1974.
[120] D. R. Scifres, R. D. Burnham, and W. Streifer, *Appl. Phys. Lett.*, vol. 25, pp. 203–206, Aug. 1974.
[121] W. S. Chang, M. W. Muller, and F. J. Rosenbaum, "Integrated optics," in *Laser Applications*, vol. 2. New York: Academic, 1974.
[122] H. F. Taylor and A. Yariv, "Guided wave optics," *Proc. IEEE*, vol. 62, pp. 1044–1060, Aug. 1974.

The Progress of Integrated Optics in Japan

YASUHARU SUEMATSU, MEMBER, IEEE

(Invited Paper)

***Abstract*—Recent progress in the field of integrated optics in Japan is reviewed. The research effort on planar guides, active integrated optics, and microoptics is outlined and pertinent references are given.**

I. INTRODUCTION

IN JAPAN, research in integrated optics appears to be accelerated by the rapid development of reliable optical components for optical communications and the expectation of wider application of optoelectronics in the future.

This paper is restricted to a summary of research activities in integrated optics in Japan. It is limited only to research but the scarcity of information given here is augmented by many references.

II. OPTICAL PLANAR GUIDES

A. Geometries and Materials

Optical planar waveguides and the question of maximum-gain conditions in a semiconductor junction laser were investigated, taking the different plasma frequencies inside and outside of the active layers into account [1].

Manuscript received April 3, 1974; revised June 18, 1974.
The author is with the Department of Electronics Engineering, Tokyo Institute of Technology, Meguro-ku, Tokyo, Japan.

The transverse-mode confinement in asymmetric thin-film dielectric guides with inhomogeneous refractive-index distributions was discussed [2], [3]. To build active devices with the help of optical dielectric waveguides, a tunable parametric oscillator was proposed. Phase matching was accomplished with the help of the mode-dependent dsipersion characteristic of the slab guide [4].

More recently, scattering caused by random imperfections in dielectric-slab waveguides was discussed in detail [5], and the modes of metal-clad dielectric guides [6] and anisotropic and gyrotropic guides [7] were investigated. A method of parameter measurements using two guided modes was applied to thin-film glass guides prepared by an RF sputtering process [8].

Ion-exchange and ion-migration methods were applied with excellent success to form guiding cores in glass plates [9], [10]. Thallium ions were diffused from the surface of the glass through a mask. Losses of these two-dimensional multimode guides were reported to be less than 0.01 dB/cm at a wavelength of 0.63 μm. Direct connection between these guides or between the guides and optical fibers was achieved with losses of less than 10 percent. Axial changes in the depth of the guiding core beneath the surface were achieved by using a spatially varying electric field to produce ion migration [11]. Diffusion of lead ions was also used to form glass guides, and focusing properties were demonstrated [12]. Many other materials